Mixed-Gas Separation in Fluorinated Polyimides: Connecting the Molecular Scale and Continuum Scales

Ravi C. Dutta and Suresh K. Bhatia*
School of Chemical Engineering, The University of Queensland, Brisbane, QLD 4072, Australia

Abstract:

We explore the temperature dependence of Maxwell-Stefan (MS) diffusivities of pure component as well as equimolar mixture of CO_2 and CH_4, in a fluorinated polyimide polymer membrane through equilibrium Molecular Dynamics (EMD) simulations. The morphology of the polymer membrane is characterized, and gas adsorption isotherms of pure as well as an equimolar mixture of CO_2 and CH_4 are extracted considering the dynamics and structural transitions in the polymer matrix upon gas adsorption, using a combination of EMD in the constant pressure ensemble and grand canonical Monte Carlo simulation. Significant swelling of the polymer in the presence of CO_2 is found, as a result of which the predictions of traditional models such as Ideal Adsorption Solution Theory and extended Langmuir model in mixed gas conditions are inaccurate, particularly for CH_4. Our results show that plasticization behavior of the polymer is observed at a CO_2 loading of 70 cc (STP)/cc of polymer, leading to increase in CO_2 permeability with increase in pressure. The Onsager coefficients indicate that in mixed gas conditions finite correlations exist between the diffusing species in the polymer membrane. Further, CH_4 is kinetically selected at high pressures in mixtures due to availability of larger pores, in contrast to pure gas conditions where CO_2 is kinetically selected over CH_4 at all pressures. Analysis of membrane behavior under practical conditions using EMD-based transport coefficients shows that while the CO_2/CH_4 selectivity increases with increase in pressure based on pure component data, the trend is opposite for mixture data. Thus, the commonly used approach of screening membrane materials based on pure component data can be misleading, as it overlooks the correlation effects that arising from the presence of other species in the mixture.

Keywords: Polymer membranes; Maxwell Stefan diffusivity, Plasticization, Gas Mixtures, Onsager Coefficients, Membrane modeling;

* To whom correspondence may be addressed. Tel.: +61 7 3365 4263. Email: s.bhatia@uq.edu.au.

1. Introduction

The understanding of molecular transport in a dense polymer matrix is an important problem of long standing interest and crucial to the design of several industrial processes for gas separation and purification, dialysis, pervaporation and reverse osmosis.[1, 2] Gas permeation through a polymer membrane is explained in terms of a solution-diffusion mechanism,[3] and involves both solubility and diffusivity differences that are strongly related to the thermodynamic properties of the polymer at a given temperature and pressure. Screening of membrane materials for a given application is often based on pure component data; however, the performance of a membrane for the separation of a given gas pair in mixed gas conditions can differ significantly from that of pure gas conditions, due to competitive sorption as well as plasticization/swelling behavior of the polymer.[4-6] In addition, the driving force for diffusion of a species in a mixture is not only provided by the gradient of the chemical potential of that particular component, but also by the gradient in the chemical potential of the other components. An understanding of mixture transport is therefore critical to gas separation processes.

The transport behavior of a species in a multicomponent environment can be described using several equivalent mathematical expressions.[1, 7] The Onsager formalism, considering chemical potential gradient ($-\nabla\mu$) as driving force, provides a fundamental approach based on irreversible thermodynamics, in which the flux (N_i) is expressed as:

$$N_i = \sum_j L_{ij}(-\nabla\mu_j) \tag{1}$$

where L_{ij} is the symmetric matrix of Onsager transport coefficients. An equivalent mathematical expression based on concentration gradient (∇c) as driving force, the generalized Fick's law, can be written as,[8]

$$N_i = \sum_j D_{ij}.(-\nabla c_j) \tag{2}$$

where D_{ij} is the multicomponent Fickian diffusion coefficient and can take both positive and negative values. Further, the cross coefficients are typically not equivalent *i.e.* $D_{ij} \neq D_{ji}$. A more convenient approach, often used to represent multicomponent transport in membrane materials, the Maxwell-Stefan (MS) formalism, considers a balance between chemical potential gradient and frictional force experienced by a species *i* with the other species in the mixture, and is expressed as:

$$-\frac{1}{RT}\nabla\mu_i = \sum_{\substack{j=1 \\ j\neq i}}^{n} \frac{x_j(u_i - u_j)}{Đ_{ij}} + \frac{u_i}{Đ_i};\ i = 1,2,...n; \tag{3}$$

where u_i and u_j are the average velocities of species *i* and *j* respectively, *R* is the universal gas constant, and *T* is temperature. $Đ_{ij}$ represents the interaction between species *i* and *j* in the mixture and $Đ_i$ is the MS diffusivity of species *i*. Further, the Onsager reciprocal relations demand

$$Đ_{ij} = Đ_{ji} \tag{4}$$

Pure and mixed gas permeation through polymeric membranes has been extensively investigated experimentally. Most of these investigations determine diffusion coefficients of a species by considering the driving force as the concentration gradient of that species only.[4, 9-12] The correlations between the species can be evidenced experimentally from PFG-NMR studies, [13, 14] but this does not provide any quantitative information regarding the exchange coefficients ($Đ_{ij}$). Further, in mixed gas conditions, the matrix of diffusivities depends on the concentrations of all the diffusing species, and its experimental characterization is therefore challenging and not straightforward. On the other hand, atomistic simulations can aid in extracting these correlations and can play an important role as a complement to experiments. Krishna et al.[8, 14-19] extensively investigated mixture diffusion in inorganic membrane materials such as zeolites and found that

correlation effects are strong functions of pore concentration, topologies and nature of the mixture. Recently, Krishna[20] analyzed literature experimental data and reported that cross correlations between the diffusing species are extremely significant in polymer membranes. However, there is scant information regarding the correlations between mixture gas molecules, and to the best our knowledge extensive simulations of mixture transport in polymer membrane materials are yet to be reported. In then literature, investigations have been largely devoted to pure component systems.[21, 22] While some work on O_2/N_2 mixture diffusion in a 6FDA-6FpDA polyimide membrane has been reported[23], the analysis is based on a Fickian interpretation of the transient gas uptake using MD, and the binary nature of the transport remains to be addressed.

On the other hand, while gas adsorption characteristics of glassy polymers in pure and mixed gas conditions has been extensively studied experimentally,[24-26] interest in the *in-silico* investigations of gas adsorption in polymers considering the structural transition upon gas adsorption is relatively recent.[21, 22, 27, 28] Pandiyan et al.[29] studied the sorption and desorption of CO_2 in a variety of fluorinated polyimides, and found significant and homogeneous swelling during the sorption. Hölck et al.[30] studied the sorption behavior of gases in a glassy polymer under conditions leading to maximum and no swelling of the polymer, and proposed a model to describe the gas sorption based on linear combination of the corresponding isotherms, that was in agreement with their experimental results. Our recent simulations considering the structural transition and redistribution of voids upon gas adsorption in BDPA-APB polyimide[21], offer a more accurate alternative for the single component case, but have yet to be extended for mixtures. On the other hand, mixture adsorption in polymers has been predicted from pure component data,[31] by applying ideal adsorbed solution theory (IAST) [32] that has been reported to be accurate for inorganic membrane materials. However, the validity of the predictions in polymers is not clear due the inherent assumptions on

which this theory was developed, such as a rigid host matrix. Here, we implemented a two-step methodology combining Grand canonical Monte Carlo simulations (GCMC) coupled with NPT (constant number of particles, pressure and temperature) EMD simulations to determine gas adsorption isotherms in pure and mixed gas conditions.

In the work reported here, we investigate the pure and mixed gas transport properties of CO_2 and CH_4 in a commercially used glassy polymeric membrane material, 6FDA-durene. The presence of $–C(CF_3)_2–$ and a bulky methyl group in the polymer backbone contributes to the reduction of local segmental mobility and inhibits the inter chain packing, resulting in a great amount of free volume and thereby good gas separation performance. To the best of our knowledge this is the first report of the MS diffusivities and adsorption isotherms of gases in pure and mixed gas conditions in 6FDA-durene polyimide polymer membrane through EMD simulations. Further, an important aspect of this study is to predict the membrane performance in practical scenarios by solving the MS equations for a given membrane thickness and driving force, from the simulation based microscopic diffusivities and adsorption characteristics.

2. Model System and Simulations

2.1. Model

Our model system comprises of 15 flexible 6FDA-durene polyimide chains, as depicted in Figure 1, in which we investigate the adsorption and transport of pure component and equimolar (1:1) mixture of CO_2 and CH_4. In what follows we describe the model and the corresponding interaction potential parameters used in the simulations.

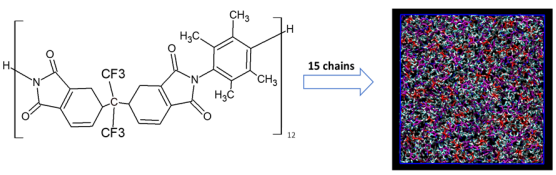

Figure 1. Structure of 6FDA-durene polyimide polymer membrane.

2.1.1. Polymer Model

The model polymer system is composed of 15 flexible polyimide polymer chains, each having 12 monomers of 6FDA-durene (4,4′-(hexafluoroisopropylidene) diphthalic anhydride, 2,3,5,6-tetramethyl-1,4-phenylenediamine) and was generated by following a self-avoiding random walk technique using Packmol.[33] The polymer chains were described by considering a combination of appropriate bonded and non-bonded interactions with all atom representation, where all the atoms in the system are defined explicitly based on the polymer consistent force field (PCFF).[34] This ab initio force field has been widely used to model long chain molecules.[21, 30, 35-37] The non-bonded van der Waals (vdW) interactions are incorporated using a Lennard–Jones (LJ) potential of the form:

$$U_{ij}^{non-bond} = \sum_{i,j} \varepsilon_{ij} \left[2\left(\frac{\sigma_{ij}}{r_{ij}}\right)^{9} - 3\left(\frac{\sigma_{ij}}{r_{ij}}\right)^{6} \right] \quad (5)$$

where ε_{ij} and σ_{ij} are the energy and length scale parameters of the LJ potential. The bonded interactions were incorporated by considering the constraints for bond, angle, dihedral, out of-plane angle and the cross-coupling terms including bod-bond, bond-angle etc., as detailed in eq (S1) of Supporting Information.

2.1.2. Adsorbate interactions

The 3-site (EPM2) linear model[38] having a point-charge on each site, explicitly accounting for the quadrupole was chosen to represent CO_2. CH_4 was represented by its full atomistic (5-site) model[39] where all the atoms having partial charge are explicitly included. The gas molecules are treated as rigid in the entire simulation, and the non-bonded van der Waals (vdW) interactions

between the gas-gas and polymer- gas molecules are incorporated using a 12-6 LJ potential of the form:

$$U_{ij}^{non-bond} = 4\varepsilon_{ij}\left[\left(\frac{\sigma_{ij}}{r_{ij}}\right)^{12} - \left(\frac{\sigma_{ij}}{r_{ij}}\right)^{6}\right] + \frac{q_i q_j}{r_{ij}} \quad (6)$$

The potential parameters are given in the Supporting Information (Table ST1) and Lorentz−Berthelot rules were used to obtain the corresponding interaction parameters.

2.2 Simulation details

EMD simulations were performed using the LAMMPS[40] package with a Nose´-Hoover thermostat and Berendsen barostat for temperature and pressure control respectively. In all the simulations, a cutoff distance of 1.4 nm was used for both potential energy and electrostatic interaction calculations. Long-range electrostatic interactions were corrected by the Ewald summation method. The Verlet method with a time step of 1 fs was used to integrate the particle equations of motion. Periodic boundary conditions (PBC) have been imposed in all three dimensions as the simulation box was considered to be a representative volume element. The simulations were run for 40 ns in the NVT ensemble with 10 ns allowed for equilibration. The results of several independent runs, each starting from a different initial configuration, were averaged to compute the gas diffusivity. The initial configurations were prepared by randomly placing the gas molecules in the polymer matrix based on the adsorption isotherm data, and allowing the polymer to swell in the presence of gas molecules for 25 ns in a NPT ensemble. The standard deviation of the results was calculated by dividing the total simulation run into four equal parts and using it to determine the statistical uncertainties associated with the simulations. In the figures to follow the error bars are smaller than the size of the symbols, unless stated otherwise.

2.3 Methodology

2.3.1. Gas adsorption isotherms and solubility

To compute the isotherms for gas adsorption, we implemented a two step procedure accounting for structural transition upon gas adsorption, as described in detail elsewhere.[22] In step-1, GCMC simulations were performed using the DL_MONTE simulation package,[41] in which the adsorbed gas is in phase equilibrium with the ambient gas phase, considering a rigid polymer matrix. In step-2, the polymer was allowed to swell in the presence of gas molecules at a given temperature and pressure by performing EMD simulations in an isobaric-isothermal ensemble for 1 ns. This procedure was repeated 5-10 times. The averages the over last 3 runs were considered to compute the adsorbed gas concentration. The error in the adsorption isotherm was determined from the last 3 GCMC runs by dividing them into 6 blocks and calculating the standard deviations with respect to the block average. Further, solubility (S_i) of gas i is evaluated from the adsorption isotherm, following:

$$S_i = \frac{c}{p_i} \tag{7}$$

where c is the amount of gas adsorbed in the polymer at its partial pressure p_i.

2.3.2. Diffusion coefficients

To describe the gas diffusion in 6FDA-durene polymer membrane, MS diffusivities are computed using the procedure described below. For pure component diffusion, the MS diffusivity is proportional to the corrected diffusivity (D_o),[19] and that D_o can be extracted from EMD simulations using an Einstein relationship, based on the center of mass (COM) motion of all adsorbed molecules, following:

$$D_o = \frac{1}{6N}\lim_{t\to\infty}\frac{1}{t} < \| \sum_{i=1}^{N} \vec{r}_i(t) - \vec{r}_i(0) \|^2 > \tag{8}$$

where $r_i(t)$ is center of mass position vector of molecule i at time t. For a binary mixture, by recasting eq (3), the MS equations can be written as,

$$-\frac{c_1}{RT}\nabla\mu_1 = \frac{x_2 N_1 - x_1 N_2}{Đ_{12}} + \frac{N_1}{Đ_1} \tag{9}$$

$$-\frac{c_2}{RT}\nabla\mu_2 = \frac{x_1 N_2 - x_2 N_1}{Đ_{12}} + \frac{N_2}{Đ_2} \tag{10}$$

However, there is no direct method to compute the MS binary exchange coefficient ($Đ_{12}$) through simulations; on the other hand, the matrix of Onsager coefficients [L_{ij}], can readily obtained from EMD simulations, following:[7, 42]

$$L_{ij} = \frac{N_i N_j}{6Vk_BT}\lim_{t\to\infty}\frac{1}{t} < [\vec{r}_i(t) - \vec{r}_i(0)].[\vec{r}_j(t) - \vec{r}_j(0)] > \tag{11}$$

where $r_i(t)$ is center of mass position vector of molecule i at time t, V is volume, k_B is Boltzmann constant, N_i is number of molecules of type i and T is temperature. These Onsager coefficients can be related to the MS diffusivities, considering the equivalence of MS formalism and Onsager formalism, following (see Supporting Information eq (S2) -(S9)):

$$Đ_1 = \frac{1}{\frac{L_{22}.c_1}{\Delta.R.T} - \frac{x_2}{Đ_{12}}} \tag{12}$$

$$Đ_{12} = \frac{R.T.\Delta}{C_T.L_{12}} \tag{13}$$

$$Đ_2 = \frac{1}{\frac{L_{11}.c_2}{\Delta.R.T} - \frac{x_1}{Đ_{12}}} \tag{14}$$

where $\Delta = L_{11}L_{22} - L_{12}L_{21}$, x_1 is mole fraction of species 1, $c_1$is concentration of species 1 and c_T is the total concentration of the species in the polymer i.e. $c_T = c_1+c_2$.

2.3.3. Membrane modelling:

The actual membrane behavior is predicted by numerically computing the steady state fluxes after a step change in the pressure, by simultaneously solving the ODEs.

$$\frac{-c_1}{P_1}\frac{dP_1}{dz} = \frac{x_2N_1 - x_1N_2}{Đ_{12}} + \frac{N_1}{Đ_1} \tag{15}$$

$$\frac{-c_2}{P_2}\frac{dP_2}{dz} = \frac{x_1N_2 - x_2N_1}{Đ_{12}} + \frac{N_2}{Đ_2} \tag{16}$$

$$\nabla.N_i = 0 \quad \text{where } i = 1,2; \tag{17}$$

All the calculations were performed on a membrane of finite thickness (δ = 30 μm), with no interfacial mass transfer resistance,[37]and maintaining the downstream at constant partial pressure (p_i=1 atm, i=1,2) with the following boundary conditions as shown in Figure 2. It is assumed that the gas phase, on both upstream and downstream sides of the membrane, consist of an equimolar mixture of CO_2 and CH_4.

Boundary conditions:

upstream conditions (at $z = 0$): $p_i=p_0$, $x_1= x_{1,0}$, $x_2=x_{2,0;}$

downstream conditions (at $z = \delta$): $p_i = p_\delta$, $x_1= x_{1,\delta}$, $x_2=x_{2,\delta;}$

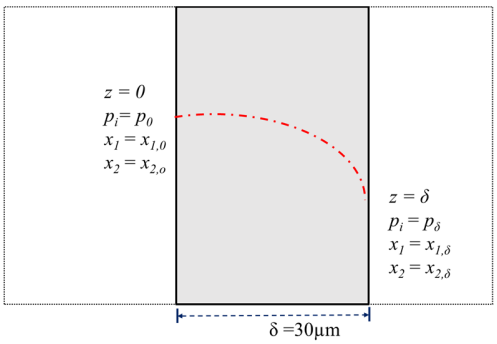

Figure 2. Schematic illustration of the 6FDA-durene polymer membrane.

2.4. Membrane performance

To determine the membrane performance for a given gas pair, its permeability as well as selectivity are calculated as defined below:

2.4.1. Permeability

The permeability (P_i) of a gas *i* in a membrane is determined by its diffusivity (D_i) and solubility (S_i), and is expressed as:

$$P_i = D_i \times S_i \tag{18}$$

In addition, the permeability can also be defined as the steady state flux (N_i) normalized by the driving partial pressure across the membrane and the membrane thickness (δ), following:

$$P_i = \frac{N_i . \delta}{\Delta p_i} \tag{19}$$

The permeabilities are expressed in Barrers, where 1 Barrer = $10^{-10} \frac{cc(stp).cm}{cm^2.s.cmHg}$.

2.4.2. Selectivity

The ideal selectivity (α_{ij}) of a gas pair *i, j* is defined as the ratio of their individual gas permeability coefficients P_i, P_j which can also be expressed in terms of contributions of the diffusivity and solubility, following:

$$\alpha_{ij} = \frac{P_i}{P_j} = \underbrace{\left(\frac{D_i}{D_j}\right)}_{\text{kinetic selectivity}} \underbrace{\left(\frac{S_i}{S_j}\right)}_{\text{adsorption selectivity}} \tag{20}$$

3. Results and Discussions:

3.1. *Characterization of polymer structure*

The ability of the force field to represent 6FDA-durene polymer membrane is illustrated by characterizing the polymer structure using volume-temperature relations, associated free volume and pore size distribution (PSD) analysis. Figure 3(a) depicts the temperature dependence of the specific volume ($1/\rho$) of 6FDA-durene polymer at 1 atm pressure. It is seen that 6FDA-durene polymer has a density of 1.34 (± 0.1) g/cc at 300 K, well in agreement with the experimental value of 1.31-1.37 g/cc.[43-45] It is observed that specific volume of the polymer increases linearly with increase in temperature with change in slope at 680 (± 10) K, the glass transition temperature (T_g) of the polymer, which compares well with the experimental value of 683-697 K.[43-45] We note here that the effect of pressure on the structure of the polymer is found to be negligible up to 30 atm, as shown in the Supporting Information (Figure S1). The inset of Figure 3(a) depicts the temperature dependence of fractional free volume (FFV) in the polymer, determined using helium as a probe molecule,[45-48] by averaging over several configurations of polymer structure at each temperature. It is seen that FFV of 6FDA-durene polymer increases linearly with increase in temperature, with change in slope at T_g of the polymer, illustrating the swelling behavior of the polymer with increase

in the temperature. We note that that 6FDA-durene polymer has a free volume of 7 (±1) % at 300 K, showing a large deviation from the experimental free volume of 18-24 %,[45] estimated using Bondi's group contribution method. This difference arises because the computed free volume neglects the contribution of sites that are not accessible to helium, while Bondi's group contribution method includes these. To confirm this, we determined the FFV of polymer using an imaginary probe of various diameters. It is seen that FFV increases with decrease in probe diameter and reaches an experimental value of ~25 % for a probe diameter of 1 Å, as shown in the Supporting Information (Figure S2). We further note that a free volume of 6% in 6FDA-durene has been reported using bulk positron annihilation lifetime spectroscopy with sodium probe,[49] in close agreement with predictions of this work. Figure 3(b) depicts the variation of accessible volume with the diameter of probe at various temperatures in 6FDA-durene polymer membrane. It is seen that pores of 3-4 Å diameter exist in the polymer membrane in the temperature range of 300-500 K, and the absence of larger pores even at higher temperatures indicates the availability of more small pores with the swelling of the polymer.

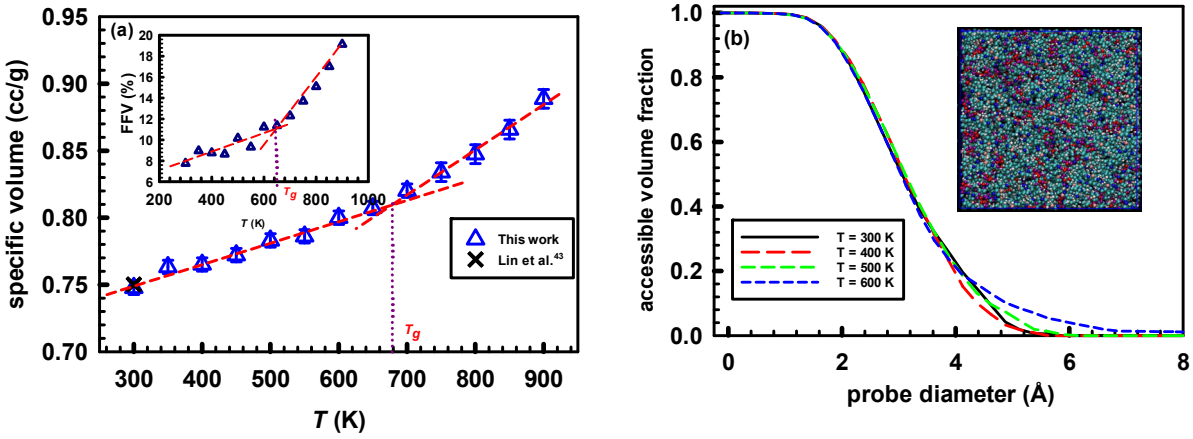

Figure 3. (a) Variation of specific volume (inset: fractional free volume) in 6FDA-durene membrane with temperature, and (b) comparison of variation of fractional accessible volume with probe diameter at various temperatures. Structure of 6FDA-durene at 300 K is depicted in the inset.

3.2. *Gas adsorption isotherms*

3.2.1. Pure component gas adsorption isotherms

The swelling behavior of 6FDA-durene polymer upon gas adsorption and its effect on gas adsorption kinetics was systematically investigated by comparing the adsorption isotherms for each adsorbed gas as a single component in a polymer, both with and without swelling on gas adsorption. A comparison of gas adsorption isotherms at 300 K in 6FDA-durene polymer for both cases is shown the in the Supporting Information (Figure S3). It is seen that the swelling behavior of the polymer influences the gas adsorption isotherms significantly. Further, the effect of swelling is more pronounced at elevated pressures owing to its high gas adsorption capacity. In addition, the effect of swelling on the polymer structure was investigated by computing the pore size distribution. It is seen that greater pore volume and larger pores are available at higher pressures. The adsorption isotherm of each gas considered was fitted using a Dual-mode (DM) sorption model of the form:

$$c = k_D p + \frac{C_H' b p}{1 + b p} \tag{21}$$

where, c is the total concentration of the sorbate in the polymer, p is the pressure, k_D is Henry's law coefficient, C_H' is the Langmuir capacity term, and b is the Langmuir affinity parameter.

Table 1. Comparison of DM sorption model fitting parameters of pure component CO_2 and CH_4 in 6FDA-durene polymer membrane.

	CO_2			CH_4		
	without swelling	with swelling	Experimental[49-51]	without swelling	with swelling	Experimental[49, 51]
C_H' (cc (STP)/cc (polyp))	32.5 (±1.0)	76 (±12.0)	61-85.0	18.1 (±0.6)	22.0 (±2.0)	38.1-39
b (atm^{-1})	19.0 (±5.0)	2.4 (±1.5)	0.66-0.80	7.0 (±1.0)	2.6 (±1.14)	0.15-0.16
k_D (cc (STP)/cc (polym).atm)	0.5 (±0.1)	4.0 (±0.7)	2.26-3.85	0.45 (±0.1)	2.0 (±0.8)	0.3-0.5

It seen that the fitting parameters C_H', b and k_D of the DM sorption model from this study considering the swelling of the polymer upon gas adsorption are in better agreement with reported values based on fits of experimental isotherms as shown in the Table1. However, we note that the parameters are sensitive to the pressure range over which the fitting is done.

Figures 4 (a)-(b) depict pure component adsorption isotherms of CO_2 and CH_4 in 6FDA-durene polymer membrane respectively, at temperatures from 300-500 K. It is seen that the CO_2 adsorbs strongly while CH_4 shows weak adsorption in 6FDA-durene polymer, and gas adsorption increases with increase in pressure at a given temperature. The adsorption capacity of both the gases decreasing with increase in temperature. The adsorption isotherm of each gas considered was fitted using DM sorption model. We note that overall sorption for both the gases is dominated by the Langmuir capacity term, as expected in polymers below glass transition temperature, as shown in Supporting Information (Figure S4).

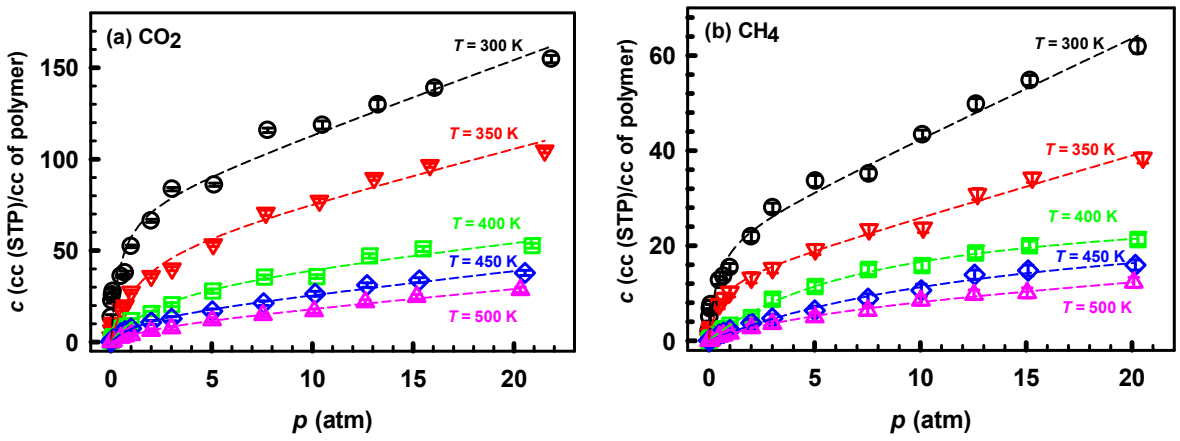

Figure 4. Pure component adsorption isotherms of (a) CO_2, and (b) CH_4 in 6FDA-durene at various temperatures. The dashed lines indicate the fitted adsorption isotherms using the dual mode sorption model.

3.2.2. Mixed gas adsorption isotherms

Although pure component isotherms are valuable for an initial screening of the materials, evaluation of adsorption isotherms in mixed gas conditions is essential to understand effects such as preferential sorption. The adsorption behavior of gases in 6FDA-durene polymer membrane in mixed gas conditions was systematically investigated by considering an equimolar (1:1) mixture of CO_2 and CH_4 the using the two-step procedure discussed in section 2.3. Figure 5 (a) depicts the adsorption isotherms of an equimolar mixture of CO_2 and CH_4 in 6FDA-durene polymer membrane at 300 K. It is seen that CO_2 adsorbs strongly while CH_4 shows weak adsorption in 6FDA-durene polymer membrane, and gas adsorption increases with increase in pressure at a given temperature. We note that the individual gas adsorption capacity in the mixed gas conditions is lower than the corresponding gas adsorption capacity in pure gas conditions at any given pressure, indicating competitive sorption is inhibiting gas adsorption to an extent and this effect is

more intense at higher pressures. The adsorption isotherm of each gas was fitted simultaneously using a DM sorption model for mixed gases, of the form:[25, 52]

$$c = k_D p_i + \frac{C_H' b_i p_i}{1 + \sum_{i=1}^{2} b_i p_i} \tag{22}$$

where, c is the total concentration of the sorbate in the polymer and p_i is the partial pressure of the component i, where k_D is Henry's law coefficient, C_H' is the Langmuir capacity term, and b_i is Langmuir affinity parameter. We note here that b_1 and b_2 are shared parameters. This model is widely used to describe mixed gas adsorption in polymers.[52] Similar plots for adsorption isotherms of equimolar mixture of CO_2 and CH_4 in 6FDA-durene polymer membrane in the range 300-500 K, are shown in Supporting Information (Figure S5).

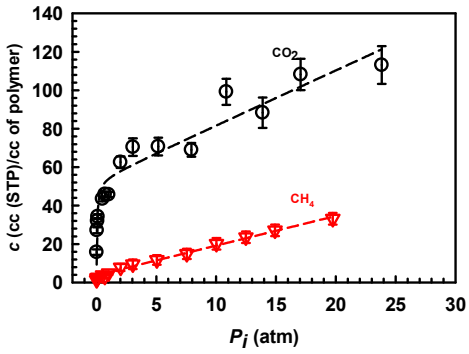

Figure 5. Adsorption isotherms of equimolar mixture of CO_2 and CH_4 in 6FDA-durene membrane at T = 300 K. The dashed lines indicate the fitted adsorption isotherms using the DM sorption model for mixed gases.

3.2.3. Solubility coefficients

Figure 6 depicts a comparison of the temperature dependence of solubility coefficients under pure and mixed gas conditions for CO_2 and CH_4 in 6FDA-durene polymer membrane at 2 atm pressure

in the temperature range of 300-500 K. At 300 K, the calculated values of solubility coefficient of CO_2 and CH_4 in pure gas conditions are 33 (± 2.0) and 10.9 (± 1.0) cc (STP)/cc (polym).atm, in good agreement with experimental values of 25 (± 3.0) and 8.2 (±1.7) cc (STP)/cc (polym).atm, respectively.[49, 53] The adsorption selectivity of CO_2 over CH_4 is found to be 3.0 (±0.2), in excellent agreement with an experimental values of 3.0-3.5.[49, 53] On the other hand, the gas solubility under mixed gas conditions is lower than that of the corresponding gas solubility in pure gas conditions. Nevertheless, preferential adsorption of CO_2 in the available Langmuir sites due to its stronger interaction with the polymer than CH_4 is evident, leading to a sharp decrease in methane solubility, and thus high adsorption selectivity of CO_2 over CH_4 in mixed gas conditions. At 300 K, the calculated values of solubility coefficient of CO_2 and CH_4 in mixed gas conditions are 31 (± 2.0) and 3.9 (± 0.5) cc (STP) / cc (polym). atm, respectively. It is seen that solubility of CO_2 and CH_4 decreases with increase in temperature, owing to decrease in gas adsorption capacity of the polymer with increase in temperature, following the van's Hoff relation,

$$S = S_0 e^{\frac{-\Delta H_s}{RT}} \tag{23}$$

where S_0 is a constant, ΔH_s is apparent, R is the gas constant and T is the temperature. Similar values of heat of solution for CO_2 in 6FDA-durene membrane in pure and mixed gas conditions (-13.0 (±1) and -13.3 (±1) kJ/mol respectively) are observed, while a decrease in heat of sorption in mixed gas conditions is observed for methane, due to less effective packing of methane molecules in the presence of CO_2. Further, the narrower, more strongly adsorbing sites are more likely to be filled by CO_2, leaving the predominantly larger sites for CH_4 in the mixed gas. We further note that negative values of ΔH_s demonstrate the exothermic nature of the adsorption process.

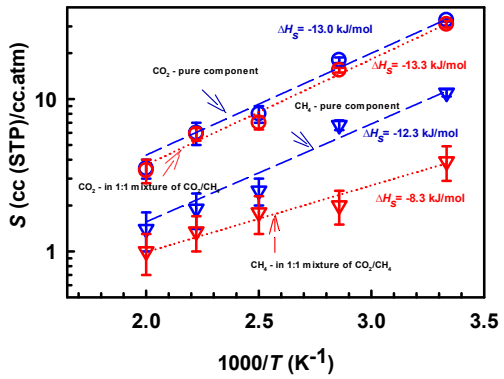

Figure 6. Temperature dependence of solubility coefficients of CO_2 and CH_4 in 6FDA-durene at 2 atm pressure in pure and mixed gas conditions.

3.2.4. Comparison of simulated adsorption isotherms with IAST predictions

The adsorption behavior of gases in mixed gas conditions can be estimated from pure component adsorption data using ideal adsorption solution theory (IAST)[32] or extended Langmuir model.[52] A comparison of simulated adsorption isotherms of an equimolar mixture of CO_2, and CH_4 in 6FDA-durene polymer membrane at 300 K with the predictions of both IAST and extended Langmuir model is depicted in Figure 7 (a) and (b), respectively. It is seen that for the more strongly adsorbed CO_2 the predictions of both IAST and the extended Langmuir model are consistent with the simulation results, while significantly large deviation between the theories and simulation results is observed for methane. This is because the swelling of the polymer in mixed gas conditions is similar to that in the presence of pure CO_2, this being the more dominant species. While IAST under predicts, the extended Langmuir model over predicts the adsorption of methane in mixed gas conditions compared to the simulation results. The large discrepancy with simulation for methane underscores the importance of accounting for structural changes in the polymer due to the presence of partner species, *i.e.* CO_2 in this case; since the system violates the hypothesis on which these theories were developed, that the adsorbing framework is inert from a thermodynamic

point of view. The foregoing results demonstrate that predictions of mixed gas adsorption using these theories in polymers can be misleading even below the plasticization pressure.

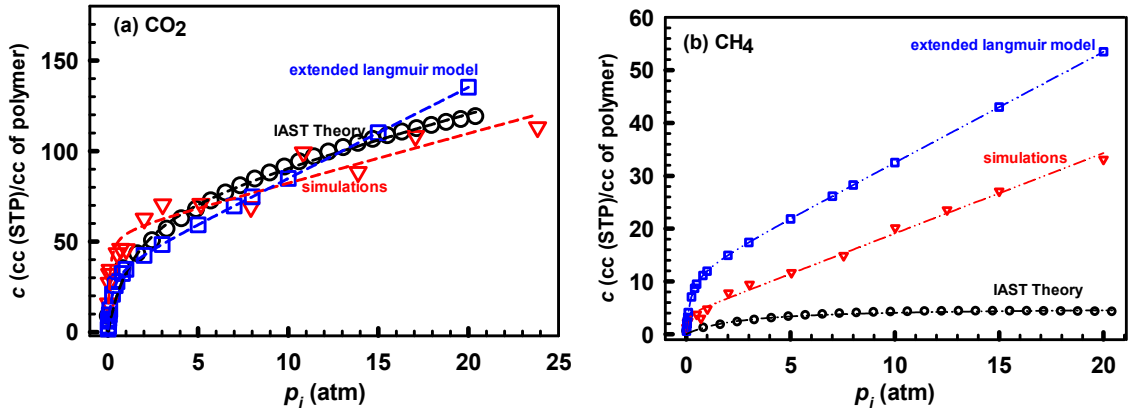

Figure 7. Comparison of simulated adsorption isotherms of equimolar mixture (a) CO_2, and (b) CH_4 in 6FDA-durene at T = 300 K with the predictions of IAST and extended Langmuir theory.

3.3. Pure-component diffusion

To understand gas diffusion behavior in the 6FDA-durene polymer membrane, the corrected diffusion coefficient of gas molecules was determined by tracking the temporal centre-of-mass motion of all the adsorbed species in the polymer matrix. Figure 8 (a) depicts the loading dependence of corrected-diffusivity of pure component CO_2 and CH_4 in the 6FDA-durene membrane at 300 K. It is seen that for methane, a moderate increase in diffusivity with increase in loading is observed, while a stronger increase in diffusivity with increase in loading, especially at high loadings, is observed for CO_2. This can be attributed to the plasticization behavior of the polymer at high CO_2 loadings. To investigate this further, the permeability of the gases at various loadings was determined, and is depicted in Figure 8 (b). It is seen that permeability of methane decreases with increase in loading, as is typical for polymers due tom the strong decrease in

solubility with pressure, while the permeability of CO_2 decreases up to about 5 atm. pressure and then increases with increase in loading. This increase in permeability with increase in pressure has also been observed experimentally[44] at around 5 atm. pressure, corresponding to the plasticization pressure of the polymer.

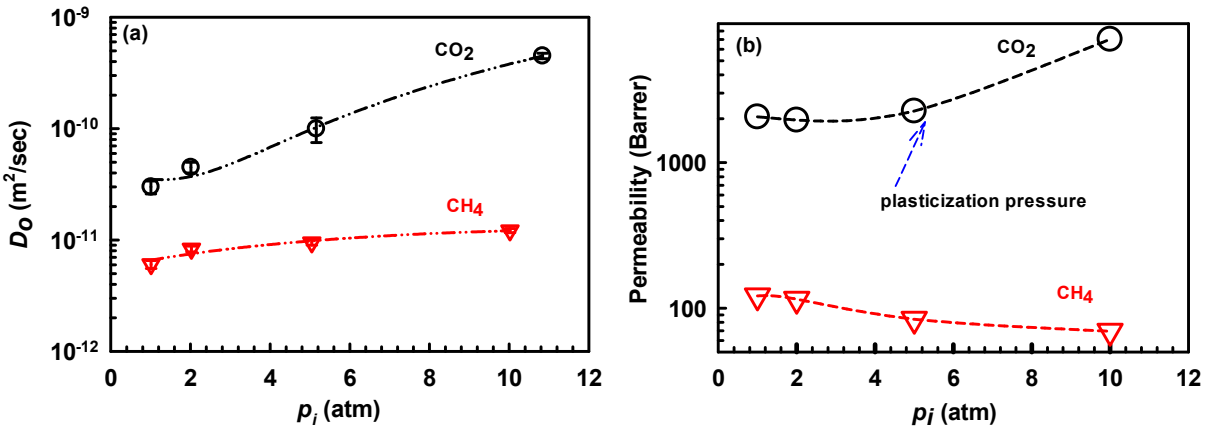

Figure 8. Loading dependence of (a) corrected diffusivity, and (b) permeability of the gases at T=300 K in 6FDA-durene membrane.

The structural changes in the polymer membrane due to plasticization can be characterized by investigating the PSD in the polymer at various gas loadings using a spherical probe of varying probe diameter through the geometric approximation technique, and are depicted in Figure 9(a)-(b). An increase in fractional accessible volume for larger probe diameters is seen at high pressures indicating the availability of larger pores due to swelling of the polymer upon gas adsorption. It is seen that 5-7 Å pores are available after swelling in the in the presence of CO_2, while 4-5 Å pores are available in the presence of CH_4, as shown in the insets of the respective figures. We note that 3-4 Å pores are available in the neat polymer membrane. The greater availability of number of larger pores in the presence of CO_2 can be attributed to plasticization behavior of the polymer at elevated pressures. The greater availability of large pores at high pressure leads to stronger increase in CO_2 diffusivity with increase in pressure.

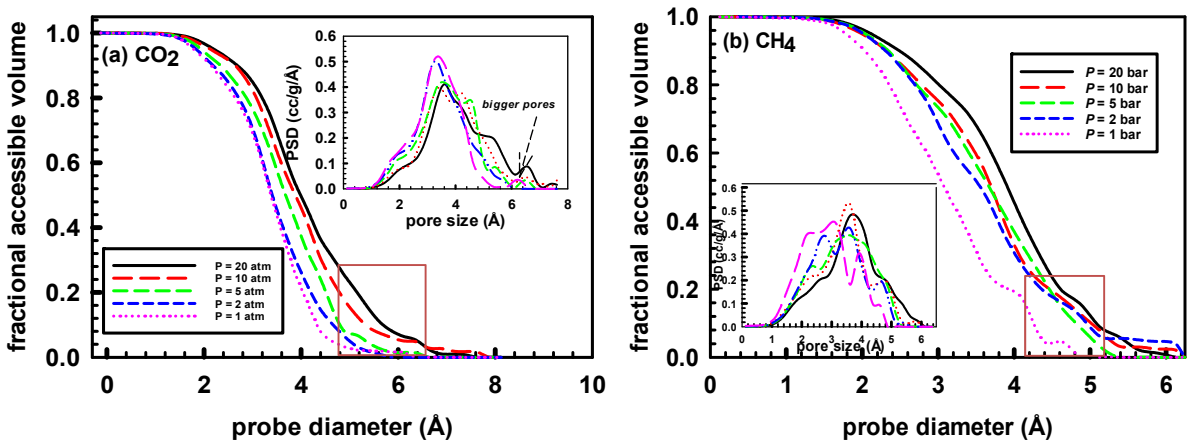

Figure 9. Comparison of variation of fractional accessible volume with probe diameter in 6FDA-durene polymer in the presence of (a) CO_2, and (b) CH_4 at various loadings. A comparison PSD at various gas loadings is depicted in the respective insets.

Figure 10 (a) depicts the temperature dependence of the corrected-diffusion coefficients of pure component CO_2 and CH_4 in a neat 6FDA-durene polymer membrane in the temperature range of 300-500 K. At 300 K, the calculated values of corrected diffusion coefficient (D_o) of CO_2 and CH_4 are 5 (± 0.5) × 10^{-11} and 0.85 (± 0.1) × 10^{-11} m^2/sec, in reasonable agreement with experimental values of 6.6 × 10^{-11} and 1.25 × 10^{-11} m^2/sec respectively.[53] The activation energies for CO_2 and CH_4 in 6FDA-durene membrane are 5 (± 2) and 10.5 (± 3) kJ/mol respectively, based on the expression,

$$D = D_0 \, e^{-E_D/RT} \tag{24}$$

where D_0 is a constant, E_D is the apparent activation energy for diffusion, R is the gas constant and T is absolute temperature. Figure 10(b) depicts the temperature dependence of the perm-selectivity of CO_2 over CH_4 in a 6FDA-durene polymer membrane in the temperature range of 300-500 K. At 300 K, the calculated values of the kinetic, adsorption and perm selectivity of CO_2 over CH_4 are 5.0, 3.0 and 15, in excellent agreement with experimental values of 5.3, 3.0 and 15.9

respectively.[53] It is seen that 6FDA-durene is selective for CO_2 over the temperature range of 300-500 K and this selectivity decreases with increase in temperature. This decrease in selectivity is due to greater increase in methane diffusivity, this being a lighter and more weakly adsorbing molecule than CO_2, which leads to a steep decrease in kinetic selectivity with increase in temperature as shown in the inset of Figure 10(b).

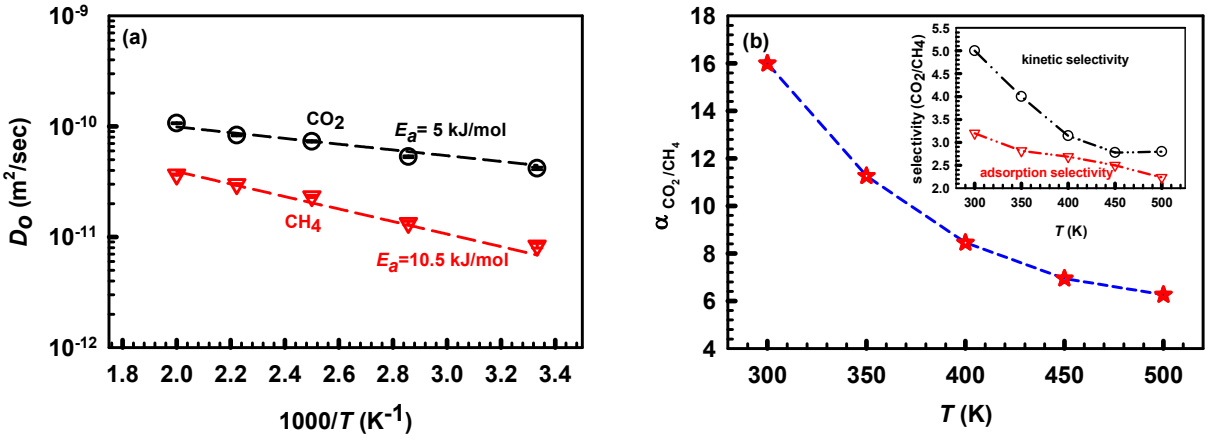

Figure 10. (a) Temperature dependence of collective diffusivity of CO_2 and CH_4 in 6FDA-durene membrane, and (b) ideal selectivity of CO_2 over CH_4 in 6FDA-durene in the temperature range of 300-500 K. A comparison of kinetic and adsorption selectivity of CO_2 over CH_4 in 6FDA-durene is depicted in the inset.

3.4. Mixture diffusion

3.4.1. Determination of Onsager coefficients

To investigate the diffusion behavior of gases in mixed gas conditions, Onsager coefficients of an equimolar mixture of CO_2/CH_4 were determined using eq (11). Figure 11 (a) depicts the variation of Onsager coefficients with pressure in a 6FDA-durene polymer membrane at 300 K. It is seen that the diagonal Onsager coefficients L_{12} (= L_{21}) are much smaller than L_{11}, but comparable to L_{22} at low pressures, while the diagonal and off diagonal elements of matrix [L] are of the same order at high pressures. Figure 11 (b) depicts the variation of Onsager coefficients with temperature in

the 6FDA-durene polymer membrane at a total pressure of 4 atm. It is seen that the diagonal Onsager coefficients L_{12} (= L_{21}) and L_{22} are quite similar to each other at all temperatures while L_{11} is an order of magnitude higher than L_{12} at low temperatures, and of the same order at high temperatures. Further, the influence of these correlations on each of the species cannot be determined from the Onsager coefficients, as these correlations influence all elements in the Onsager coefficients matrix.[54] However, the extent of coupling between the diffusing species can be determined from the Onsager coefficients.

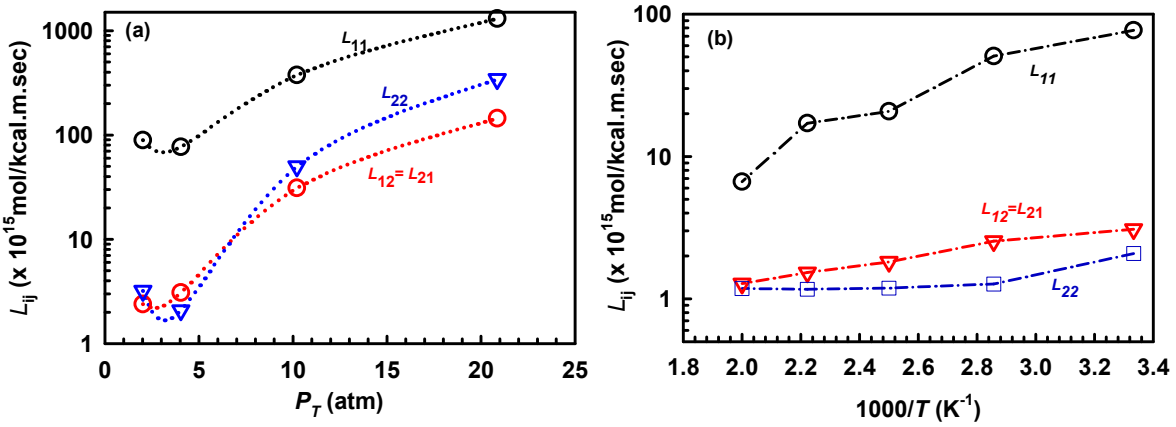

Figure 11. Variation of Onsager coefficients of an equimolar mixture of CO_2/CH_4 in 6FDA-durene membrane with (a) pressure at T = 300 K, and (b) with temperature at $p_T \sim 4$ atm

The extent of coupling can be determined by computing an interaction parameter (λ), following:[55]

$$\lambda = \frac{L_{12}}{\sqrt{L_{11}.L_{22}}} \tag{25}$$

Strong correlation between the diffusing species results in $L_{12} = \sqrt{L_{11}L_{22}}$, with $\lambda = 1$. On the other hand, weak correlation between the diffusing species, corresponding to $L_{12} \rightarrow 0$, results in $\lambda = 0$. In all other cases with finite correlations, depending on loading and nature of the adsorbate and adsorbent, λ takes a value between 0 and 1.[18] It is seen that the well known relation between

Onsager coefficients, $L_{12} = \sqrt{L_{11}L_{22}}$, does not hold for the equimolar mixture of CO_2 and CH_4 in 6FDA –durene polymer membrane, as depicted in Figure 12 (a), indicating the presence of weak or finite correlations between the diffusing species in the polymer membrane. Similar behavior is also observed in MFI zeolite that has 3-dimensional pore network with finite exchange correlations.[16] We note that that the Onsager coefficients always satisfy the relation $L_{11}L_{22} > L_{12}L_{21}$,[56] indicating the computed MS diffusivities from Onsager coefficients will only have a positive value. Figure 12 (b) depicts the variation of λ with temperature. At 300 K, the λ value is found to be 0.25, indicating the presence of finite correlation between the diffusing species in the polymer membrane, and this interaction parameter increases with increase in temperature, due to increase in CH_4 mole fraction and gas diffusivity with temperature arising from the swelling behavior of the polymer. An initial increase in λ with increase in pressure is observed, followed by slight decrease with increase in pressure after 5 atm. It is expected that the degree of correlation between the species increases with increase in loading;[14] however, we note that the mole fraction of the gases in the polymer membrane may decrease or increase with pressure, and that influences the behavior of λ with pressure.

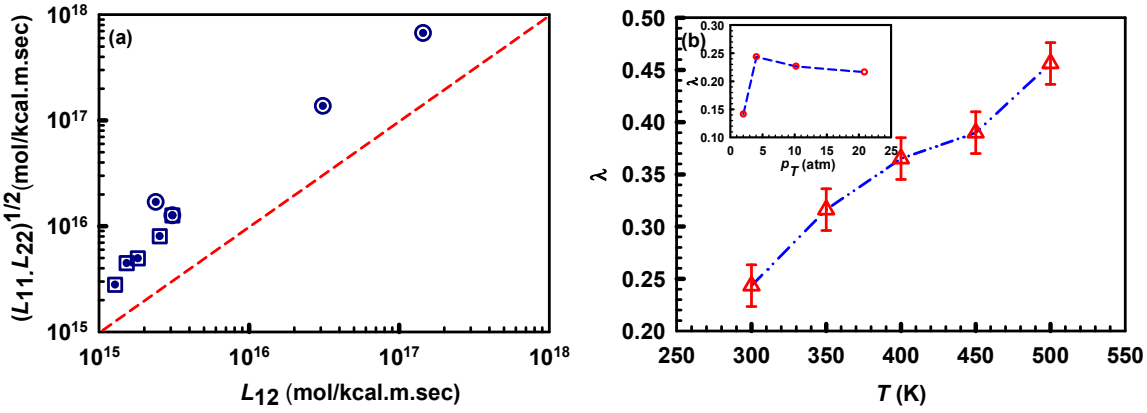

Figure 12. (a) Comparison between L_{12} and $\sqrt{L_{11}L_{22}}$ in 6FDA-durene polymer, and (b) Variation of interaction with parameter (λ) with temperature. Variation of λ with pressure at T =300K is shown in the inset.

3.4.2. Determination of MS diffusivities

The above findings indicate that gas diffusion behavior in the mixture can be different to that of the pure components due to the finite correlations that exists between the diffusing species; however, the effect of this correlation on individual species is unclear. The general understanding is that these correlations decrease the mobility of more mobile species and increase the diffusivity of slower species. To investigate this correlation effect on each of the species, the MS diffusivities were determined using eq (12)-(14). Figure 13(a) depicts the loading dependency of the MS diffusivities of an equimolar CO_2/CH_4 mixture. At low pressure, CO_2 is kinetically selective over methane, while methane is kinetically selective over CO_2 at high pressures, contrary to the pure gas conditions where CO_2 is kinetically selective over methane at all the pressures studied in this work at 300 K. This is because, at high pressures, the availability of larger pores promotes methane diffusion, this being a lighter and more weakly adsorbed molecule. It is seen that $Đ_1$, $Đ_2$ and $Đ_{12}$ are of the same order, further confirming the presence of finite degree of correlations between the diffusing species. Further, the degree of correlation is defined as $\frac{Đ_i}{Đ_{ij}}$, and $\frac{Đ_i}{Đ_{ij}} \ll 1$ and $\frac{Đ_i}{Đ_{ij}} \gg 1$ are the two limiting scenarios that represent very weak and strong correlations between the diffusing species, respectively. For CO_2, the degree of correlation, decreases with pressure, while it increases with pressure for CH_4 as shown the inset of Figure 13 (a). This is due to the fact that correlation effects are more significant to the more mobile species than for the slower species as the latter vacates the sites less frequently. Figure 13(b) depicts the temperature dependency of MS diffusivities of an equimolar mixture of CO_2 and CH_4. It is seen that CO_2 is kinetically selective over CH_4 at all temperatures. Further, the degree of correlation for both the gases increases with increase in temperature, and this can be attributed to increase in CH_4 mole fraction in the mixture with temperature as shown in the Supporting Information (Figure S6). Further, the swelling

behavior of the polymer with temperature can lead to opening up of the pore mouths, resulting in gas-gas interactions increasing in significance compared to gas-polymer interactions. Further, it is seen that $Đ_1$, $Đ_2$ and $Đ_{12}$ increase with increase in temperature following Arrhenius type behavior, with activation energies 4.9 (± 1), 7.1 (± 2) and 3.7 (± 0.5) kJ/mol, respectively, computed using eq (24). We note that CO_2 has the same activation energy in pure and mixed gas conditions, while a decrease in activation energy is observed for methane in mixed gas condition. This can be attributed to the availability of larger pores in mixed gas conditions, leading to increase in methane diffusivity compared tp the pure component value at low temperatures. As expected, the values of the degree of correlation for CO_2 are larger than those for methane as shown in inset of Figure 13 (b), due to the smaller size of the former.

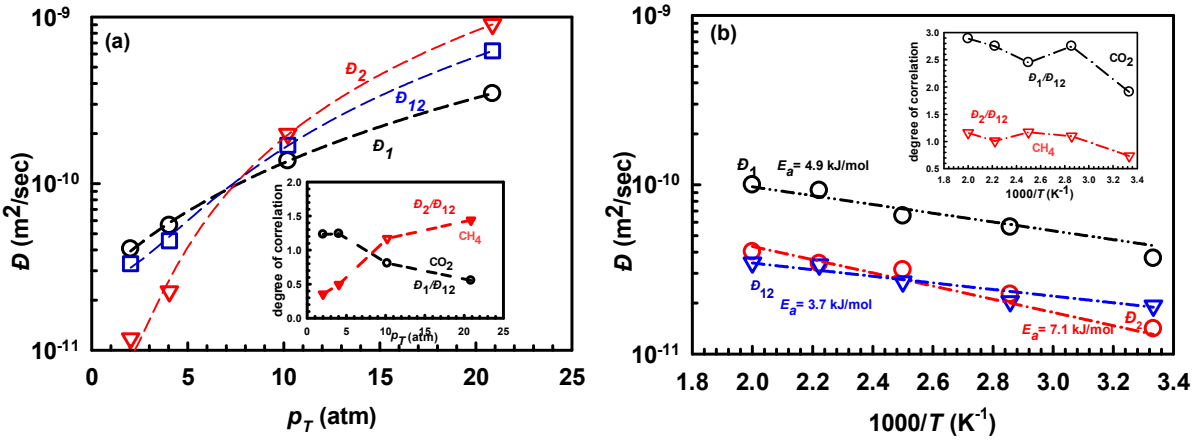

Figure 13. Variation of MS diffusivities in an equimolar mixture of CO_2/CH_4 in 6FDA-durene with (a) pressure at $T = 300$ K, and (b) with temperature at $p_i = 2$ atm.

3.5. Determination of molar flux across a membrane

To understand the gas separation characteristics of a 6FDA-durene membrane in practical scenarios, from our EMD data, we determined the molar fluxes across the membrane by solving MS equations for a given membrane thickness considering the pressure gradient as driving force.

Further, to solve the MS equations in mixed gas conditions, the reported MS diffusivities were fit to an empirical equation as a function of total pressure using a polynomial of the form,

$$Đ_i = a_0 + a_1 p + a_2 p^2 \tag{26}$$

We note here that these fits should not be used to predict MS diffusivities outside the data range. Figure 14 depicts the predicted variation in CO_2 selectivity over CH_4 with feed gas pressure in an equimolar mixture, as well as the corresponding results for the case of pure gas conditions. In mixed-gas conditions, CO_2 selectivity decreases with increase in feed gas pressure, in contrast to that for pure gas conditions, where an increase in selectivity with increase in feed gas pressure is observed. This can be attributed to the availability of larger pores in the polymer membrane due to its swelling behavior which is substantial in the presence of CO_2, leading to an increase in methane diffusivity, this being a lighter and weakly adsorbing molecule. This behavior is in agreement with the experimental findings of Donohue et al.[6] where a decrease in selectivity with increase pressure is observed in a cellulose acetate membrane due to plasticization. Further, we note that the discrepancy in the selectivity's are evident even below the plasticization pressure, however, this discrepancy is significant after the plasticization pressure. The predicted molar fluxes of the gases in pure and mixed gas conditions are summarized in the supporting Information (Table ST2). The foregoing results demonstrate that characterizing the membrane performance for a given application based on the pure component data can be deceptive, and a thorough understanding of membrane performance under realistic operating conditions are indispensable.

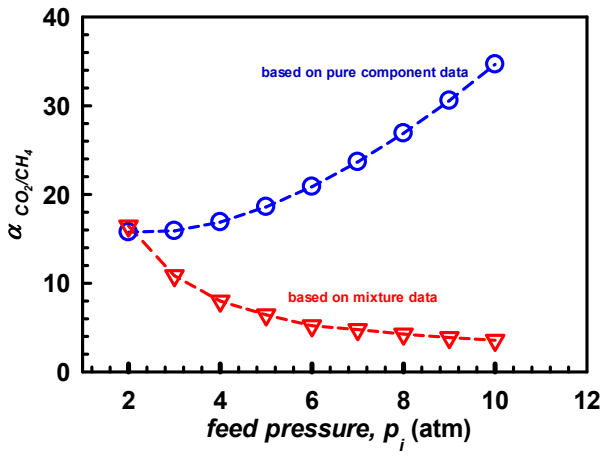

Figure 14. Comparison of variation in CO_2 selectivity over CH_4 with the feed pressure, in 6FDA-durene polymer membrane in pure and mixed gas conditions.

4. Conclusions

The Maxwell-Stefan (MS) diffusivities of CO_2 and CH_4 as pure components as well as for their equimolar mixture in the temperature range of 300-500 K in 6FDA-durene polyimide polymer membrane have been investigated here, using equilibrium molecular dynamics simulations. The structure of 6FDA-durene polymer membrane is visualized by exploring the volume-temperature relations, associated fractional free volume and pore size distributions. The swelling behavior of the polymer due to the presence of gas molecules has been investigated at the microscopic level over a wide range of temperatures. We have presented a detailed study of CO_2 and CH_4 adsorption in pure as well as mixed gas conditions in 6FDA-durene polymer membrane in the temperature range of 300 to 500 K by considering the possible swelling of the polymer and its dynamics. It is found that CO_2 is more soluble than CH_4 at all temperatures in a 6FDA-durene polymer membrane, and this solubility decreases with increase in temperature following the van't Hoff relation. In mixed gas conditions, a decrease in adsorption capacity is observed for both the gases and this

effect is more significant for methane, leading to an increase in adsorption selectivity of CO_2 over CH_4. It is seen that a 6FDA-durene polymer membrane is selective for CO_2 over CH_4. In addition, the simulated adsorption isotherms were compared with the predictions of IAST and extended Langmuir model. It is seen that for CO_2 the simulation results are consistent with the predictions of both IAST and the extended Langmuir model, while a large deviation between the theories and simulation results is observed for methane. While IAST under-predicts, the extended Langmuir model over-predicts the adsorption of methane in mixed gas conditions compared to the simulation results. The large discrepancy with simulation underscores the importance of accounting for structural changes in the polymer due to the presence of partner species, when predicting mixed gas isotherms.

Pure component diffusivities of CO_2 and CH_4 in 6FDA-durene polymer membrane are in the order of 10^{-10}-10^{-11} m^2/sec, and in good agreement with experimental reports. It is seen that the corrected diffusivities of the gases increase with increase in loading at 300 K, exhibiting a decrease in methane permeability with increase in pressure, due to swelling reducing adsorption, while an increase in CO_2 permeability with increase in pressure occurs above 5 atm, the plasticization pressure of the polymer. In addition, corrected diffusivities of the gases in 6FDA-durene polymer membrane follow Arrhenius behavior with temperature, with CO_2 being kinetically selective at all temperatures. The Onsager coefficients indicate that in mixed gas conditions, finite correlation exist between the diffusing species in the polymer membrane, and this correlation increases with increase in temperature. The MS diffusivities in the mixed gas conditions indicate that CO_2 is kinetically selective at low pressures, while CH_4 is kinetically selective at high pressures. It is also found that correlation effects are more significant to the more mobile species than for the slower species, and the degree of correlation increases with increase in temperature and is significant for

CO_2 transport at all temperatures. An important aspect of this study is the prediction of membrane behavior in practical scenarios, from EMD data, by determining the steady state flux across a membrane resulting from a pressure difference, by numerically solving the MS equations. It was found that increased feed gas pressure in mixed-gas conditions reduces CO_2 selectivity, while an increase in selectivity with increase in feed gas pressure is observed in pure gas conditions. This can be attributed to the availability of larger pores in the polymer membrane due to its swelling behavior which is substantial in the presence of CO_2, leading to an increase in methane diffusivity, this being a lighter and more weakly adsorbing molecule.

Supporting Information.

The interaction parameters used in this work, figures showing the effect of pressure on PI structure, effect of polymer swelling upon gas adsorption on the isotherms in PI are available in Supporting Information. This material is available free of charge via the Internet at http://pubs.acs.org.

Notes

The authors declare no competing financial interest.

ACKNOWLEDGMENT

This work has been supported by a grant (DP150101824) from the Australian Research Council through the Discovery scheme. This research was undertaken with the assistance of the computational resources provided at the NCI National Facility systems at the Australian National University (ANU), and those at the Pawsey Supercomputing Centre in Western Australia, through their National Computational Merit Allocation Schemes supported by the Australian Government and the Government of Western Australia.

REFERENCES

1. Strathmann, H., Membrane separation processes: Current relevance and future opportunities. *AlChE J.* **2001,** *47* (5), 1077-1087.

2. Geankoplis, C., *Transport processes and separation process principles (includes unit operations)* Prentice Hall Press: Upper Saddle River, NJ 07458, 2003; Vol. 4, p 1056.

3. Wijmans, J. G.; Baker, R. W., The solution-diffusion model: a review. *J. Membr. Sci.* **1995,** *107* (1), 1-21.

4. Ribeiro, C. P.; Freeman, B. D.; Paul, D. R., Pure- and mixed-gas carbon dioxide/ethane permeability and diffusivity in a cross-linked poly(ethylene oxide) copolymer. *J. Membr. Sci.* **2011,** *377* (1), 110-123.

5. Visser, T.; Koops, G. H.; Wessling, M., On the subtle balance between competitive sorption and plasticization effects in asymmetric hollow fiber gas separation membranes. *J. Membr. Sci.* **2005,** *252* (1), 265-277.

6. Donohue, M. D.; Minhas, B. S.; Lee, S. Y., Permeation behavior of carbon dioxide-methane mixtures in cellulose acetate membranes. *J. Membr. Sci.* **1989,** *42* (3), 197-214.

7. Sholl, D. S., Understanding Macroscopic Diffusion of Adsorbed Molecules in Crystalline Nanoporous Materials via Atomistic Simulations. *Acc. Chem. Res.* **2006,** *39* (6), 403-411.

8. Taylor, R.; Krishna, R., *Multicomponent Mass Transfer*. John Wiley & Sons, Inc.: New York, NY, 1993; Vol. 1, p 579.

9. Raharjo, R. D.; Freeman, B. D.; Paul, D. R.; Sanders, E. S., Pure and mixed gas CH4 and n-C4H10 permeability and diffusivity in poly(1-trimethylsilyl-1-propyne). *Polymer* **2007,** *48* (25), 7329-7344.

10. Raharjo, R. D.; Freeman, B. D.; Paul, D. R.; Sarti, G. C.; Sanders, E. S., Pure and mixed gas CH4 and n-C4H10 permeability and diffusivity in poly(dimethylsiloxane). *J. Membr. Sci.* **2007,** *306* (1), 75-92.

11. Reijerkerk, S. R.; Nijmeijer, K.; Ribeiro, C. P.; Freeman, B. D.; Wessling, M., On the effects of plasticization in CO2/light gas separation using polymeric solubility selective membranes. *J. Membr. Sci.* **2011,** *367* (1), 33-44.

12. Sadrzadeh, M.; Shahidi, K.; Mohammadi, T., Effect of operating parameters on pure and mixed gas permeation properties of a synthesized composite PDMS/PA membrane. *J. Membr. Sci.* **2009,** *342* (1), 327-340.

13. Fernandez, M.; Kärger, J.; Freude, D.; Pampel, A.; van Baten, J. M.; Krishna, R., Mixture diffusion in zeolites studied by MAS PFG NMR and molecular simulation. *Microporous Mesoporous Mater.* **2007,** *105* (1), 124-131.

14. Krishna, R.; van Baten, J. M., Maxwell–Stefan modeling of slowing-down effects in mixed gas permeation across porous membranes. *J. Membr. Sci.* **2011,** *383* (1), 289-300.

15. Krishna, R.; van Baten, J. M., Describing Mixture Diffusion in Microporous Materials under Conditions of Pore Saturation. *J. Phys. Chem. B* **2010,** *114* (26), 11557-11563.

16. Skoulidas, A. I.; Sholl, D. S.; Krishna, R., Correlation Effects in Diffusion of CH4/CF4 Mixtures in MFI Zeolite. A Study Linking MD Simulations with the Maxwell−Stefan Formulation. *Langmuir* **2003,** *19* (19), 7977-7988.

17. Krishna, R.; van Baten, J. M., Diffusion of Alkane Mixtures in Zeolites: Validating the Maxwell−Stefan Formulation Using MD Simulations. *J. Phys. Chem. B* **2005,** *109* (13), 6386-6396.

18. Krishna, R.; van Baten, J. M., Onsager coefficients for binary mixture diffusion in nanopores. *Chem. Eng. Sci.* **2008,** *63* (12), 3120-3140.

19. Krishna, R., Multicomponent surface diffusion of adsorbed species: a description based on the generalized Maxwell—Stefan equations. *Chem. Eng. Sci.* **1990,** *45* (7), 1779-1791.

20. Krishna, R., Using the Maxwell-Stefan formulation for highlighting the influence of interspecies (1−2) friction on binary mixture permeation across microporous and polymeric membranes. *J. Membr. Sci.* **2017,** *540*, 261-276.

21. Dutta, R. C.; Bhatia, S. K., Structure and Gas Transport at the Polymer–Zeolite Interface: Insights from Molecular Dynamics Simulations. *ACS Appl. Mater. Interfaces* **2018,** *10* (6), 5992-6005.

22. Dutta, R. C.; Bhatia, S. K., Transport Diffusion of Light Gases in Polyethylene Using Atomistic Simulations. *Langmuir* **2017,** *33* (4), 936-946.

23. Neyertz, S.; Brown, D., Air Sorption and Separation by Polymer Films at the Molecular Level. *Macromolecules* **2018,** *51* (18), 7077-7092.

24. Sanders, E. S.; Koros, W. J.; Hopfenberg, H. B.; Stannett, V. T., Pure and mixed gas sorption of carbon dioxide and ethylene in poly(methyl methacrylate). *J. Membr. Sci.* **1984,** *18*, 53-74.

25. Sanders, E. S.; Koros, W. J., Sorption of CO2, C2H4, N2O and their binary mixtures in poly(methyl methacrylate). *J. Polym. Sci., Part B: Polym. Phys.* **1986,** *24* (1), 175-188.

26. Mukaddam, M.; Litwiller, E.; Pinnau, I., Pressure-dependent pure- and mixed-gas permeation properties of Nafion®. *J. Membr. Sci.* **2016,** *513*, 140-145.

27. Spyriouni, T.; Boulougouris, G. C.; Theodorou, D. N., Prediction of Sorption of CO_2 in Glassy Atactic Polystyrene at Elevated Pressures Through a New Computational Scheme. *Macromolecules* **2009,** *42* (5), 1759-1769.

28. Wang, L.; Zhou, H.; Wang, X.; Mi, J., Modeling Solubility and Interfacial Properties of Carbon Dioxide Dissolved in Polymers. *Ind. Eng. Chem. Res.* **2016,** *55* (4), 1126-1133.

29. Pandiyan, S.; Brown, D.; Neyertz, S.; van der Vegt, N. F. A., Carbon Dioxide Solubility in Three Fluorinated Polyimides Studied by Molecular Dynamics Simulations. *Macromolecules* **2010,** *43* (5), 2605-2621.

30. Hölck, O.; Böhning, M.; Heuchel, M.; Siegert, M. R.; Hofmann, D., Gas sorption isotherms in swelling glassy polymers—Detailed atomistic simulations. *J. Membr. Sci.* **2013,** *428*, 523-532.

31. Lu, W.; Yuan, D.; Sculley, J.; Zhao, D.; Krishna, R.; Zhou, H.-C., Sulfonate-Grafted Porous Polymer Networks for Preferential CO2 Adsorption at Low Pressure. *J. Am. Chem. Soc.* **2011,** *133* (45), 18126-18129.

32. Myers, A. L.; Prausnitz, J. M., Thermodynamics of mixed-gas adsorption. *AlChE J.* **1965,** *11* (1), 121-127.

33. Martínez, L.; Andrade, R.; Birgin, E. G.; Martínez, J. M., PACKMOL: A package for building initial configurations for molecular dynamics simulations. *J. Comput. Chem.* **2009,** *30* (13), 2157-2164.

34. Sun, H.; Mumby, S. J.; Maple, J. R.; Hagler, A. T., An ab Initio CFF93 All-Atom Force Field for Polycarbonates. *J. Am. Chem. Soc* **1994,** *116* (7), 2978-2987.

35. Jiang, Q.; Tallury, S. S.; Qiu, Y.; Pasquinelli, M. A., Molecular dynamics simulations of the effect of the volume fraction on unidirectional polyimide–carbon nanotube nanocomposites. *Carbon* **2014,** *67* (Supplement C), 440-448.

36. Zhang, L.; Hu, Z.; Jiang, J., Metal–Organic Framework/Polymer Mixed-Matrix Membranes for H2/CO2 Separation: A Fully Atomistic Simulation Study. *J. Phys. Chem. C* **2012,** *116* (36), 19268-19277.

37. Dutta, R. C.; Bhatia, S. K., Interfacial barriers to gas transport in zeolites: distinguishing internal and external resistances. *Phys. Chem. Chem. Phys.* **2018,** *20* (41), 26386-26395.

38. Harris, J. G.; Yung, K. H., Carbon Dioxide's Liquid-Vapor Coexistence Curve And Critical Properties as Predicted by a Simple Molecular Model. *J. Phys. Chem.* **1995,** *99* (31), 12021-12024.

39. Sun, Y.; Spellmeyer, D.; Pearlman, D. A.; Kollman, P., Simulation of the solvation free energies for methane, ethane, and propane and corresponding amino acid dipeptides: a critical test of the bond-PMF correction, a new set of hydrocarbon parameters, and the gas phase-water hydrophobicity scale. *J. Am. Chem. Soc.* **1992,** *114* (17), 6798-6801.

40. Plimpton, S., Fast Parallel Algorithms for Short-Range Molecular Dynamics. *J. Comput. Phys.* **1995,** *117* (1), 1-19.

41. Purton, J. A.; Crabtree, J. C.; Parker, S. C., DL_MONTE: a general purpose program for parallel Monte Carlo simulation. *Mol Simul.* **2013,** *39* (14-15), 1240-1252.

42. Bhatia, S. K.; Nicholson, D., Modeling Mixture Transport at the Nanoscale: Departure from Existing Paradigms. *Phys. Rev. Lett.* **2008,** *100* (23), 236103.

43. Lin, W.-H.; Vora, R. H.; Chung, T.-S., Gas transport properties of 6FDA-durene/1,4-phenylenediamine (pPDA) copolyimides. *J. Polym. Sci. B Polym. Phys.* **2000,** *38* (21), 2703-2713.

44. Jusoh, N.; Yeong, Y. F.; Lau, K. K.; M. Shariff, A., Enhanced gas separation performance using mixed matrix membranes containing zeolite T and 6FDA-durene polyimide. *J. Membr. Sci.* **2017,** *525*, 175-186.

45. Nafisi, V.; Hägg, M.-B., Gas separation properties of ZIF-8/6FDA-durene diamine mixed matrix membrane. *Separation and Purification Technology* **2014,** *128*, 31-38.

46. Sarkisov, L.; Harrison, A., Computational structure characterisation tools in application to ordered and disordered porous materials. *Mol. Simul.* **2011,** *37* (15), 1248-1257.

47. Gelb, L. D.; Gubbins, K. E., Pore Size Distributions in Porous Glasses: A Computer Simulation Study. *Langmuir* **1999,** *15* (2), 305-308.

48. Gelb, L. D.; Gubbins, K. E., Characterization of Porous Glasses: Simulation Models, Adsorption Isotherms, and the Brunauer−Emmett−Teller Analysis Method. *Langmuir* **1998,** *14* (8), 2097-2111.

49. Japip, S.; Wang, H.; Xiao, Y.; Shung Chung, T., Highly permeable zeolitic imidazolate framework (ZIF)-71 nano-particles enhanced polyimide membranes for gas separation. *Journal of Membrane Science* **2014,** *467*, 162-174.

50. Japip, S.; Liao, K.-S.; Chung, T.-S., Molecularly Tuned Free Volume of Vapor Cross-Linked 6FDA-Durene/ZIF-71 MMMs for H2/CO2 Separation at 150 °C. *Adv. Mater.* **2017,** *29* (4), 1603833.

51. Cheng, S.-X.; Chung, T.-S.; Wang, R.; Vora, R. H., Gas-sorption properties of 6FDA–durene/1,4-phenylenediamine (pPDA) and 6FDA–durene/1,3-phenylenediamine (mPDA) copolyimides. *J. Appl. Polym. Sci.* **2003,** *90* (8), 2187-2193.

52. Koros, W. J., Model for sorption of mixed gases in glassy polymers. *J. Polym. Sci.,: Polym. Phys.* **1980,** *18* (5), 981-992.

53. An, H.; Lee, A. S.; Kammakakam, I.; Sang Hwang, S.; Kim, J.-H.; Lee, J.-H.; Suk Lee, J., Bromination/debromination-induced thermal crosslinking of 6FDA-Durene for aggressive gas separations. *J. Membr. Sci.* **2018,** *545*, 358-366.

54. Krishna, R., Describing the Diffusion of Guest Molecules Inside Porous Structures. *J. Phys. Chem. C* **2009,** *113* (46), 19756-19781.

55. Sundaram, N.; Yang, R. T., Binary diffusion of unequal sized molecules in zeolites. *Chem. Eng. Sci.* **2000,** *55* (10), 1747-1754.

56. Wang, Y.; LeVan, M. D., Mixture Diffusion in Nanoporous Adsorbents: Equivalence of Fickian and Maxwell−Stefan Approaches. *J. Phys. Chem. B* **2008,** *112* (29), 8600-8604.

Table of Contents Graphic

Mixed-Gas Separation in Fluorinated Polyimides: Connecting the Molecular Scale and Continuum Scales

Ravi C. Dutta and Suresh K. Bhatia*

School of Chemical Engineering, The University of Queensland, Brisbane, QLD 4072, Australia